



# Hybrid composite wires for tensile armours in flexible risers

**DOI:**

[10.1016/j.compstruct.2016.04.004](https://doi.org/10.1016/j.compstruct.2016.04.004)

## Document Version

Accepted author manuscript

[Link to publication record in Manchester Research Explorer](#)

## Citation for published version (APA):

Gautam, M., Potluri, P., Katnam, K-B., Jha, V., Leyland, J., Latto, J., & Dodds, N. (2016). Hybrid composite wires for tensile armours in flexible risers: Manufacturing and mechanical characterisation. *Composite Structures*, 150, 73-83. <https://doi.org/10.1016/j.compstruct.2016.04.004>

## Published in:

Composite Structures

## Citing this paper

Please note that where the full-text provided on Manchester Research Explorer is the Author Accepted Manuscript or Proof version this may differ from the final Published version. If citing, it is advised that you check and use the publisher's definitive version.

## General rights

Copyright and moral rights for the publications made accessible in the Research Explorer are retained by the authors and/or other copyright owners and it is a condition of accessing publications that users recognise and abide by the legal requirements associated with these rights.

## Takedown policy

If you believe that this document breaches copyright please refer to the University of Manchester's Takedown Procedures [<http://man.ac.uk/04Y6Bo>] or contact [uml.scholarlycommunications@manchester.ac.uk](mailto:uml.scholarlycommunications@manchester.ac.uk) providing relevant details, so we can investigate your claim.



## Accepted Manuscript

Hybrid Composite Wires for Tensile Armour in Flexible Risers: Manufacturing and Mechanical Characterisation

M. Gautam, P. Potluri, K.B. Katnam, V. Jha, J. Leyland, J. Latto, N. Dodds

PII: S0263-8223(16)30234-3

DOI: <http://dx.doi.org/10.1016/j.compstruct.2016.04.004>

Reference: COST 7368

To appear in: *Composite Structures*

Received Date: 11 March 2016

Accepted Date: 1 April 2016



Please cite this article as: Gautam, M., Potluri, P., Katnam, K.B., Jha, V., Leyland, J., Latto, J., Dodds, N., Hybrid Composite Wires for Tensile Armour in Flexible Risers: Manufacturing and Mechanical Characterisation, *Composite Structures* (2016), doi: <http://dx.doi.org/10.1016/j.compstruct.2016.04.004>

This is a PDF file of an unedited manuscript that has been accepted for publication. As a service to our customers we are providing this early version of the manuscript. The manuscript will undergo copyediting, typesetting, and review of the resulting proof before it is published in its final form. Please note that during the production process errors may be discovered which could affect the content, and all legal disclaimers that apply to the journal pertain.

## Hybrid Composite Wires for Tensile Armours in Flexible Risers: Manufacturing and Mechanical Characterisation

M. Gautam<sup>1</sup>, P. Potluri<sup>1\*</sup>, K. B. Katnam<sup>2</sup>, V. Jha<sup>3</sup>, J. Leyland<sup>3</sup>, J. Latto<sup>3</sup> and N. Dodds<sup>3</sup>

<sup>1</sup>Northwest Composite Centre, School of Materials, University of Manchester, M1 3NJ, UK

<sup>2</sup>School of Mechanical, Aerospace and Civil Engineering, University of Manchester, M13 9PL, UK

<sup>3</sup>GE Oil & Gas, Newcastle upon Tyne, NE6 3PF, UK

### Abstract

With the rising global demand for hydrocarbon fuels, there is a growing need for the oil and gas industry to operate in deeper offshore waters. In this context, the traditional metallic tensile armours in flexible risers pose certain limitations (e.g. weight, corrosion, fatigue damage) in demanding service environments. This paper presents a novel and proprietary hybrid composite wire as an alternative to metallic (carbon steel) wires. The hybrid composite wire consists of an over-braided (Dyneema<sup>®1</sup> fibres) core, with the core consisting of hexagonally packed composite rods (pultruded carbon fibre and vinyl ester). These hybrid composite wires can provide high tensile strength and stiffness accompanied by low flexural and torsional rigidities, which can easily be tailored by varying geometrical and manufacturing parameters. This paper presents the manufacturing methods used, and the mechanical behaviour of the hybrid composite wires with various configurations.

**Keywords:** Flexible risers, tensile armour wires, pultrusion, braiding, flexural rigidity, torsional rigidity

### 1. Introduction

Flexible risers have successfully been in use in the oil and gas industry since 1970 [1]. However, as the industry continues its efforts in exploring deeper offshore oil and gas reservoirs, there is a growing need for innovation in the design and manufacture of flexible risers [2, 3]. A flexible riser which carries fluids from the seabed to floating units can be described as a composite structure or pipe consisting of helically-wound metallic wires as pressure and tensile armours that are interlayered with polymeric sheaths.

Flexible risers are highly deformable and compliant in flexural modes, yet provide a strong and stiff response to internal/external pressure, tension and torsion [4]. The function of each layer in a typical flexible riser is portrayed in Fig. 1, where the tensile armour is an integral part consisting of metallic wires with rectangular

---

\*Corresponding author: Prasad.potluri@manchester.ac.uk

<sup>1</sup> Dyneema is a trademark of DSM

cross-section (filleted at the edges). These wires are wound in two or four layers, between lay angles of 20° and 55°, for resisting tensile, flexural and torsional loads [1, 5, 6]. Major failures in a flexible riser are often driven by the damage and failure of tensile armours [7] which include crack nucleation, tensile fatigue, radial buckling, and lateral buckling. Metallic armour wires may develop a hard and textured microstructure during the manufacturing stage, leading to the formation of small marks and pits. These regions can cause cracks and lead to progressive failure, which can significantly shorten the life of the component [8]. Carbon steel is the most widely used material for tensile armour wires. However, as high strength carbon steel grades are more prone to hydrogen sulphide-induced stress cracking [9], so the amount of and therefore mass of carbon steel to be used depends upon the service environment and conditions. In this regard, an alternative material and design approach that can overcome the limitations of traditional metallic tensile armour wires is sought after.

Recent works [10-13] have shown great potential for carbon fibre thermoplastic and thermoset matrix composites in replacing metallic tensile and hoop armours. These composites show higher tensile strength and fatigue, excellent corrosion resistance, and enable significant overall weight reduction of flexible riser systems. However for tensile armour, continuous manufacturing processes to produce the materials in the required long helix are not well developed. Subsequently, initial applications have involved bending and twisting linear pultrusions in the pipe structure. This inevitably imposes strain on the wire, limiting the usable thickness and resistance to brittle damage/fracture. Although the use of composites as tensile armour wires is still being developed, there are a range of offshore applications already employing composites: manufacturing of rigid risers, tethers, floors and platforms for above sea facilities, casings, J-tubes etc. [14].

This paper introduces a novel tensile armour wire design in the form of a hybrid composite, which aims to provide lower torsional and flexural rigidities whilst maintaining the high tensile stiffness and strength associated with traditional armour wires. The hybrid composite wire consists of carbon and vinyl ester circular section pultruded rods, stacked in the form of hexagonal closed packing, completely unbonded with each other but held together by over-braided ultra-high molecular weight polyethylene (UHMW-PE) fibres (commercially known as Dyneema). The Dyneema fibres used in the study are 10 times stronger than steel and 50% stronger than aramid fibres [15]. The composite rods (with unidirectional fibres) were produced using a linear pultrusion process which offers the best productivity/cost ratio among the class of composite manufacturing techniques [16]. The braiding process that has been used to bind the composite rods together, is a branch of textile manufacturing that is capable of producing near net shape preforms [17]. Braiding involves interlacing of the

yarns or tows (untwisted strands of fibres) in the bias direction. The bias angle also referred to as the braid angle, can be varied per its end application. The braiding process is also widely being used in the aerospace, automotive, marine, and textiles industries [18]. The fabrication technique used in hybrid composite wires is different from the 'braiding' process, which involves over-braiding of a core, consisting of unidirectional fibres being fed into the pultrusion process. The combination of the braiding and pultrusion process can help in the continuous production of tensile armour wires in comparison to metallic wires that are limited in supply.

In this paper, the manufacturing process and mechanical properties (i.e. flexural and torsional rigidities) of some hybrid composite wire configurations have been studied (as shown in Fig. 2). Geometric parameters of composite rods and over-braid were varied to determine an optimum configuration for the hybrid composite wire by varying individual rod diameter (2 mm and 4 mm), braid angle ( $30^\circ$ ,  $45^\circ$ , and  $55^\circ$ ), and braid topology (diamond and regular). The effect of the edge boundary condition upon flexural rigidity of the wires has also been studied and is presented in this paper in order to determine the flexural behaviour of the wires, near and away from the pipe end fittings. The effect of varying point load on the flexural behaviour of wires has also been studied.

## 2. Hybrid composite wires: manufacturing

### 2.1. Materials

Pultruded composite rods with unidirectional carbon fibres and vinyl ester matrix were used in the manufacture of hybrid composite wires. Circular pultruded rods of  $\Phi$  2 mm and  $\Phi$  4 mm, supplied by Exel Composites, were employed in the study. The mechanical properties of the materials used are given in Table 1. The mechanical properties of pultruded rods were experimentally determined using ASTM D3916 [19]; however, the properties of UHMW-PE fibres (tow) were obtained from the manufacturer's technical data sheet.

### 2.2. Over-braiding process

The over-braiding process used to manufacture hybrid composite wires is shown in Fig. 3. Pultruded rods with the same diameter (either  $\Phi$  2 mm or  $\Phi$  4 mm) were hexagonally packed (comprising seven rods). This form of packing provides the highest packing efficiency, and densest packing for straight cylinders when their axes are parallel [20]. This form of packing also extends the interaction of energy between the rods [21] and geometrically all the pairs of neighbouring axes are located at a constant distance from each other. Prior to the braiding process, the packed rods were taped at the ends and no adhesive was used to bond the rods together.

Hybrid composite wires with different configurations were manufactured with varying braid topology and braid angles. For over-braiding the hexagonally packed rods, regular (2/2) and diamond (1/1) braid topologies were used, and three different braid angles (30°, 45° and 55°) were employed. The braid angle (bias angle) for a braid can be varied for any given core diameter by changing the take-up speed or the rotational speed of the machine. The interlacement of a braided structure, which determines the topology of a braid, depends upon the number of bobbins involved in producing that braid. If a bobbin is removed from the machine, the interlacement of that yarn through the braid pattern is removed. The over-braiding of the hexagonal pack of  $\Phi$  2 mm rods was carried out by using a 24 carrier braiding machine. A diamond (1/1) braid topology was obtained (as shown in Fig. 3(a)) by employing only 12 carriers. Furthermore, the hexagonal pack of  $\Phi$  4 mm rods were over-braided by using 24 and 48 carrier braiding machines. All 24 carriers on the 24 carrier machine were used to produce a regular (2/2) braid topology (as shown in Fig. 3(b)); and only 24 carriers on a 48 carrier machine were employed to obtain a diamond (1/1) braid topology (as shown in Fig. 3 (b)). These two configurations were considered to study the effect of braid topology on the mechanical properties (i.e. flexural and torsional rigidities) of hybrid composite wires.

In order to study and compare the flexural and torsional behaviour of the hybrid wires with the hexagonal pack of  $\Phi$  2 mm rods and of  $\Phi$  4 mm rods, the same range of braid angles (30°, 45° and 55°) were chosen that resulted in full braid coverage and also avoided braid distortion or jamming. The lowest achievable braid angle of 28° provided 99.5% braid cover for both the packs (i.e. with  $\Phi$  2 mm and  $\Phi$  4 mm rods) and the highest braid angle achievable, without any distortion or jamming of the braid, was 57°. The range of braid angles employed (30°, 45° and 55°) in the study was thus within this range (i.e. between 28° and 57°). Moreover, the carrier tension was maintained at 150 grams during braiding for all the specimens.

### 2.3. Braid structural parameters

The braid structural parameters: braid angle, braid thickness, braid tow width, and braid crimp are given in Table 2. It was observed that the braid thickness increased with increasing braid angle, while the tow width decreased with increasing braid angle for the hybrid wires of  $\Phi$  2 mm and  $\Phi$  4 mm rods. As the perimeter of the tow in a braid remains the same at any given braid angle, the braid thickness and the tow width are interdependent such that an increase in the tow thickness leads to a decrease in the tow width and vice versa. The crimp phenomenon in a braid refers to the waviness or undulation of a tow as a result of interlacement between tows. Crimp for a braid can be quantified as the ratio of the difference between the length of the

crimped tow ( $L_c$ ) and the length of the un-crimped tow ( $L_{uc}$ ) to that of the length of the crimped tow ( $L_c$ ). The braid crimp percentage ( $C$ ) for all the configurations of braided specimens was calculated using Eq. 1.

$$C = \frac{(L_{uc} - L_c)}{L_c} \times 100 \quad (1)$$

As shown in Table 2, for both hybrid wires of  $\Phi$  2 mm and  $\Phi$  4 mm rods, an increase in braid angle led to an increase in braid crimp. For the hexagonal pack with  $\Phi$  2 mm rods, an increase in crimp of 56% and 35% was observed as the braid angle was increased from 30° to 45° and further to 55°. However, in relation to the hexagonal pack with  $\Phi$  4 mm rods, as the braid angle was increased from 30° to 45°, braid crimp increased by 12% for diamond braid and 38% for regular braid. As the braid angle was further increased from 45° to 55°, the braid crimp increased by 79% for diamond braid and 52% for regular braid. This trend of increase in braid crimp with an increase in braid angle was due to the increase in braid density, which increases as more tows are deposited per unit length. The crimp value will also be at a minimum when the braid angle is closer to 0°, and maximum when the braid angle is closer to 90° [22].

The effect of braid topology on braid crimp was also found to be significant for 30° and 55° braid angle where a decrease in braid crimp of 18% for 30° braid angle and a further decrease of 14% for 55° braid angle, was observed as the topology was changed from diamond to regular. However, for 45° braid only a small decrease in braid crimp of about 0.8% was observed as braid topology was changed from diamond to regular. For diamond and regular braid produced using the same number of tows, the same length of tow in a regular braid will experience lower crimp compared to the diamond braid due to its higher float length.

### 3. Mechanical tests procedure

#### 3.1 Flexure tests

Since there were no specific standards for testing a material or structure similar to the hybrid wire, from the available standards [23-25] related to fibre reinforced composite materials, ASTM D7264 [25] was used as it contained test procedures for both three point and four point flexural tests. The four point flexural test was chosen over the three point flexural test, as the bending moment remains constant between the two inner point loads and most importantly it gives a better representation of the flexural behaviour of hybrid wire bent around the pipe.

In order to determine the flexural properties of hybrid wires, and the individual rods, four-point flexural tests were performed for two types of edge boundary condition. In the first type of edge boundary condition, the specimens were taped within 10 mm at both ends using high performance tape, depicting the flexural behaviour of long lengths of armour wires. In the second edge boundary condition, the edges at both ends of the specimens were bonded together by the application of a structural adhesive. The structural adhesive was applied within 10 mm at both ends, depicting the flexural behaviour of armour wires near the end fittings of the riser. The first type of boundary condition was investigated for all configurations of hybrid wires. For the second type of edge boundary condition only one configuration was chosen for hybrid wires with  $\Phi$  4 mm rods.

For the flexural tests, 5 specimens each of all configurations of specimens were tested, with span to thickness ratio of 32:1, where the span length of 176 mm was used for packing with  $\Phi$  2 mm rods, and a span length of 352 mm was chosen for packing with  $\Phi$  4 mm rods. For individual rods, there already exists a standard [26] to test circular pultruded rods however, it is only applicable for the three-point flexural test and requires a different test fixture. Therefore, the same test standard of ASTM D7264 [25] was followed to for testing single rods. The span length of 64 mm was used for the  $\Phi$  2 mm rod and the  $\Phi$  4 mm rod span length of 128 mm was used. The hybrid wires containing  $\Phi$  4 mm rods could only be tested to the maximum of  $\sim 2\%$  strains equivalent to 55 mm flexural deflection due to the limitations of the test rig. However, hybrid wires containing  $\Phi$  2 mm rods, were tested up to  $\sim 4\%$  global strain equivalent to 55 mm deflection as depicted in Fig. 4. The results have only been reported till 2% strains to compare with hybrid wires containing  $\Phi$  4 mm rods.

As the hybrid wires are a combination of multiple unbonded structures, it is a non-homogenous material. Therefore, in order to rectify the flexural properties obtained using a four point flexural test, a three point flexural test was additionally carried out using ASTM D7264 [25], with the same span to thickness ratio of 32:1 that was used for the four point flexural test. Only 3 specimens were tested for each type of structure until  $\sim 1\%$  strain for hybrid wires with  $\Phi$  4 mm rods and diamond braid topologies. The test was carried out merely to compare the elastic properties with already obtained values from the four point flexural test. The flexural strain ( $\epsilon_f$ ) was calculated using Eq. 3, defined in ASTM D7264 [25] as the maximum strain at the surface of a specimen occurring at mid-span, which can be calculated with the help of mid-point deflection ( $\delta_{max}$ ) measured using a video extensometer, specimen thickness ( $h$ ) and the span length ( $L$ ). The cross-head speed of 5 mm/min as recommended in the standard was used with the maximum capacity of a load cell of 10kN.



$$EI = M/\kappa \quad (2)$$

$$\varepsilon_f = 4.36 \delta_{max} h / L^2 \quad (3)$$

$$\kappa = 2\varepsilon_f / h \quad (4)$$

The flexural rigidity of an isotropic structure can be quantified by the product of tensile modulus ( $E$ ), and area moment of inertia ( $I$ ). As the hybrid wire is not isotropic material, its flexural rigidity was calculated experimentally from the slope of the flexural moment ( $M$ ) versus curvature ( $\kappa$ ), defined in Eq. 2, between 1000-3000  $\mu\epsilon$  as per ASTM D7264 [25]. The curvature of a structure subjected to flexural loads was calculated from specimen thickness ( $h$ ), and flexural strain ( $\varepsilon_f$ ) as defined in Eq. 4.

### 3.2. Torsion tests

The torsion tests as represented in Fig. 5, were carried out to the maximum limit of 400°/m (40° twist angle), with a gauge length of 100 mm, for hybrid wires, with  $\Phi$  2 mm rods and  $\Phi$  4 mm rods. Five specimens of each type of structure were tested. As the hybrid wire was twisted, the exterior rods in the packed structure wrapped around the centre rod generating complex strain components for both the braid and the composite rods. As the aim of the conducted test was merely to determine shear behaviour of the structure as a whole, the value of the angle of twist was itself obtained from the load cell rotation by assuming the packed rods with and without braid as a homogenous material. Moreover, the application of the strain gauge onto the braid would damage the braid and distort the braid angle.

Since there was no available standard to test a structure with a cross-section similar to hybrid wire (hexagonal with filleted edges) comprising multiple unbonded materials, two different approaches were used to determine the effective technique for holding the rods and the braid together in the clamped region during the torsion test. In the first approach, hybrid wires were coated within 20 mm at both ends with Araldite 2000+ epoxy based resin and hardener mixture, and then inserted in cylindrical aluminium pots used as tabs, also containing the same resin and hardener mixture. In the second approach, the aluminium pots were not used as tabs. However, the rods and the braid were bonded together within 20 mm of both ends using the same resin and hardener mixture as the first approach. V-grips were used to maximize the grip at the ends ensuring no slippage would occur during the test. The lowest possible cross-head rotation speed of 1°/sec was used providing greater accuracy of the results. The first approach resulted in very high deviation within the same type of specimens tested, due to the aluminium tabs that crushed under grip leading to slippage and entanglement with the braid

during the test. The second approach yielded a much lower deviation within the same type of specimen tested, due to absence of aluminium tabs. Only the results from the second technique have been reported in this paper.

The load cell used for torsion tests had a capacity of 1000 N-m whereas, the maximum load achieved for hybrid wires, was almost 1/100<sup>th</sup> of the maximum capacity. The accompanying noise in the curves was more pronounced for hybrid wires with  $\Phi$  2 mm rods. Since the noise for each specimen was consistent, linear and non-linear fitting of the curves was carried out using Origin software. Due to the high level of noise generated (limitation of load cell), the single rods with  $\Phi$  2 mm and  $\Phi$  4 mm, were also tested under torsion to 400°/m twist per length, but with a lower gauge length of 50 mm (lesser noise), to compare the shear behaviour of a single rod with different configurations of hybrid wires. The twist angle for single rods was also determined using cross-head rotation as the application of strain gauge was not feasible due to high curvature of the rods.

$$GJ_p = T/(\theta/L) \quad (5)$$

Torsional rigidity for an isotropic structure can be quantified by the product of its shear modulus ( $G$ ) and its polar moment of inertia ( $J_p$ ). However, as the hybrid wire is not an isotropic material, the torsional rigidity was calculated experimentally from the slope of torque ( $T$ ) versus twist per length ( $\theta/L$ ) curve, as depicted in Eq. 5, obtained from [27]. The shear behaviour for all configurations of specimen tested is depicted in Fig. 5. The torsional rigidity for all configurations of tested specimen was determined from the slope of torque and twist per length, between 1000-6000  $\mu\epsilon$  conforming to both ranges specified in ASTM D3518 [28] (1500 - 4000  $\mu\epsilon$ ) and ASTM D5448 [29] (1000 - 6000  $\mu\epsilon$ ).

#### 4. Mechanical characterisation

##### 4.1 Flexural rigidity

Flexural rigidity helps to define the rigidity of the material used during the test, irrespective of span length. Since the span length differed for packs with different diameter rods and for single rods, flexural rigidity is a useful tool to compare the flexural behaviour of different specimens as it is independent of the span length used.

The normalised flexural rigidity values of hybrid wires, with respect to individual rods used in their packing has been shown in Fig. 6.

If the flexural rigidity of a single rod is compared with hybrid wire, the flexural rigidity of hybrid wires with  $\Phi$  2 mm rods and  $\Phi$  4 mm rods was found to be between 7-9 times the rigidity of the single rod used in its packing. The higher flexural rigidity for hybrid wire was due to the higher area moment of inertia (Eq. 2). The effect of a

single rod diameter in the packing was also found to be highly significant. The flexural rigidity of hybrid wires with  $\Phi$  4 mm rods was found to be approximately 16 times the flexural rigidity of hybrid wires containing  $\Phi$  2 mm rods for all three braid angles of  $30^\circ$ ,  $45^\circ$ , and  $55^\circ$  each with diamond braid topology, due to a higher second moment of inertia.

The effect of braid angle on the flexural rigidity was found to be less significant, with a maximum standard deviation (within the same single rod diameter and topology) in the flexural rigidity of  $0.01 \text{ Nm}^2$  for hybrid wires with  $\Phi$  2 mm rods, and a maximum standard deviation of  $0.13 \text{ Nm}^2$  for hybrid wires with  $\Phi$  4 mm rods. Experimentally, the minor change in the flexural rigidity due to the change in braid angle remained inconclusive, which could be due to the dry nature of the braid. When the braid is impregnated with resin, its effect is more pronounced, and an increase in the braid angle leads to a decrease in flexural rigidity as presented in [30]. The flexural rigidity of the hybrid wires with regular braid was expected to be higher due to a lower crimp value (Table 2) as compared to diamond braid topology, resulting in higher tenacity of the tows.

The flexural behaviour of hybrid wires with  $\Phi$  2 mm rods can be observed in Fig. 7, where none of the braided specimens underwent any form of failure. The effect of the braid angle on the flexural rigidity of the hybrid composite wires was found to be insignificant up to  $4.5 \text{ m}^{-1}$  ( $\sim 0.22 \text{ m}$  radius of curvature) where the wires at all three braid angles of  $30^\circ$ ,  $45^\circ$ , and  $55^\circ$  showed similar flexural rigidities (shown in Fig. 7). However, beyond  $4.5 \text{ m}^{-1}$  curvature all three braid angles showed inelastic behaviour. Similar flexural behaviour was observed in the braided specimen with  $\Phi$  4 mm rods, for both diamond and regular braid topologies. The effect of both braid angle and braid topologies upon the flexural rigidity of wires was found to be less significant. The elastic behaviour was observed up to approx.  $2.25 \text{ m}^{-1}$  curvature ( $\sim 0.44 \text{ m}$  radius of curvature). However, beyond the curvature of  $2.25 \text{ m}^{-1}$  all three braid angles of  $30^\circ$ ,  $45^\circ$ , and  $55^\circ$  wires showed inelastic behaviour.

The inelastic behaviour for both types of wires with  $\Phi$  2 mm rods, and  $\Phi$  4 mm rods was most pronounced in the  $30^\circ$  braid angle (as shown in Fig. 8) for wires with  $\Phi$  4 mm rods that underwent packing deformation reducing the area moment of inertia and effective flexural rigidity of the structure. The higher braid angles of  $45^\circ$  and  $55^\circ$  did not depict any packing deformation, where inelastic response was also observed, which could be due to the combined effect of geometric and material non linearity. The inelastic behaviour could also be a result of inter-rod interaction inside the packing during high flexural loads. The highest bending moment value was observed in the  $55^\circ$  braid angle, followed by the  $45^\circ$  and  $30^\circ$  braid angles. The  $55^\circ$  angle, having the

densest braid and strongest grip on the hexagonally-packed rods increased the overall flexural rigidity of the structure.

Flexural behaviour in single rods is presented in Fig. 4, where both single rods with  $\Phi$  2 mm and  $\Phi$  4 mm experienced failure due to the fibres splitting. The single rod with  $\Phi$  2 mm showed greater fibre splitting in the region between the load pins due to tensile (bottom face of rod) and compressive forces (upper face of the rod). The rod with  $\Phi$  4 mm showed fracture with permanent deformation at the point of contact with the load pins, due to the action of compressive forces on the surface. However, no major fibre splitting between the load pins was observed; this was more pronounced for rod with  $\Phi$  2 mm. Both single rods tested failed within the elastic region, unlike the wires that showed a non-linear response. This infers that the packing aids in imparting inelastic behaviour to the unidirectional composites subjected to both tensile and compressive forces during flexural deformation, that otherwise (single rod) did not show inelastic behaviour.

#### 4.1.1 Effect of boundary conditions

Two types of boundary conditions, one with taped edges and one with bonded edges were investigated for both hybrid wires and packed rods without braid (shown in Fig. 9). The pack rods without braid and taped edges, started to deform within  $2 \pm 0.5$  mm of the cross-head displacement. Whereas, the packed rods without braid and bonded edges, depicted similar behaviour as compared to specimens with taped edges (pack deformation), post bond failure, which occurred within  $8 \pm 1$  mm of cross-head displacement. In case of hybrid wires ( $2/2$ ,  $45^\circ$ ), the bond failure occurred at  $8 \pm 0.8$  mm cross-head displacement between the rods, and a second bond failure at  $11 \pm 0.5$  mm, between braided fibres and rods. The flexural rigidity of bonded edged specimen was found to be almost twice to that of the specimens with taped edges, for both hybrid wires and packed rods with no braid. No packing deformation was observed for either of bonded and taped edged hybrid wires.

#### 4.1.2 Effect of point load

To determine the effect of point loads, an additional three point flexural test were carried out. The flexural rigidity for the four point and three point flexural tests were calculated from the slope of the bending moment versus curvature, between 1500 to 3000  $\mu\epsilon$  as per ASTM 7264 [25]. The effect of the braid angle for diamond braid on flexural rigidity remained insignificant as shown in Fig. 10. On comparing the flexural rigidity obtained from the three point and four point flexural tests, maximum standard deviation of  $\pm 0.35 \text{ Nm}^2$  was observed. The

small change in flexural rigidity is an indicator that increasing or decreasing number of loading points would only result in a small change in the flexural rigidity of hybrid wires.

#### 4.2 Torsional rigidity

The normalised torsional rigidity of all configurations of specimens tested is presented in Fig. 6, where significant effects on torsional rigidity by variation of braid angle, braid topology, and packing thickness were observed. The torsional rigidity of hybrid wires with  $\Phi$  2 mm rods, was found to be 8.5 to 10.5 times the torsional rigidity of its individual rod. While the torsional rigidity of hybrid wires (including diamond and regular braids) with  $\Phi$  4 mm rods, was found to be between 13.5 to 15.6 times the torsional rigidity of single rod used in its packing. The higher flexural rigidity for hybrid wire was due to the higher area moment of inertia (Eq. 5). The effect of the rod diameter upon the torsional rigidity of hybrid composite wires was found to be highly significant such that as the diameter of rods was doubled from 2 mm to 4 mm, an increase of 1941% for  $30^\circ$ , 1712% for  $45^\circ$  and 1784% for  $55^\circ$  braid angle was noted due to the higher second moment of inertia.

As the braid angle was increased from  $30^\circ$  to  $45^\circ$ , torsional rigidity increased approximately 22% for braided packing with  $\Phi$  2 mm rods with diamond braid topology. When the braid angle was further increased from  $45^\circ$  to  $55^\circ$  a decrease in torsional rigidity of about 11.5% was observed. For the hybrid wires with  $\Phi$  4 mm rods and diamond braid topology, an increase in torsional rigidity of 9% was observed as the braid angle was increased from  $30^\circ$  to  $45^\circ$ . However, as the braid angle is further increased from  $45^\circ$  to  $55^\circ$  a decrease in torsional rigidity of 8% was observed. The highest torsional rigidity of  $45^\circ$  braid conforms to the trend observed among composite laminates predicted by composite laminate theory [31] which predicts the highest in-plane shear modulus ( $G_{12}$ ) by  $45^\circ$  ply orientation followed by  $30^\circ$  and  $55^\circ$  ply orientations. A study conducted in [32] to determine the effect of braid angle upon torsional properties of biaxial braided composite tubes,  $45^\circ$  specimens showed the highest shear modulus among two other braid angles of  $31^\circ$  and  $65^\circ$ . In addition, in a study conducted in [30] on braided pultruded composites,  $45^\circ$  braided specimens showed the highest shear modulus followed by  $30^\circ$  and  $55^\circ$  braided specimens.

The hybrid wires with  $\Phi$  4 mm rods and regular braid also showed similar behaviour. When the braid angle was increased from  $30^\circ$  to  $45^\circ$ , an increase in torsional rigidity of 2.5% was observed while a decrease of 9% was observed when the braid angle was further increased from  $45^\circ$  to  $55^\circ$ . The torsional rigidity of hybrid wires with  $\Phi$  4 mm rods with regular braid for all three braid angles investigated was observed to be higher than diamond braid topology. When the braid topology was changed from diamond to regular an increase in torsional rigidity

of 19% at 30°, 13% at 45°, and 12% at 55° braid angle was observed. This increase in torsional rigidity can be explained using the braid crimp which is higher in the case of the diamond braided specimens (depicted in Table 2) providing greater extensibility and displaying lower rigidity than the regular braided specimens when the same number of bobbins is employed for producing the braid.

As observed in Fig. 11, none of the specimens underwent any failure. Among both types of hybrid wires, the highest torsional rigidity (slope) and torque value at maximum twist angle was portrayed by a 45° braid angle followed by 30° and 55° braid angles. The ability of 45° braid to resist shearing of the braided tows imparts it at the highest torsional rigidity. The hybrid wires with  $\Phi$  2 mm, depicted linear behaviour while hybrid wires with  $\Phi$  4 mm rods depicted non-linear behaviour to the maximum test limit of 400°/m. If the effect of topology is observed, the hybrid wires with regular braid depicted the highest torsional rigidity (slope) and the torque value at maximum twist angle, for all three braid angles, as compared with hybrid wires with diamond braid topology. The hybrid wires with 55° braid angle with diamond braid topology and  $\Phi$  4 mm rods showed an increase in torsional rigidity with an increase in twist angle, though at a decreasing rate.

All other braid configurations of hybrid wires with  $\Phi$  4 mm rods depicted a concavo–convex curve (with reference to x axis). Such a curve implies an increase in torsional rigidity with an increase in twist angle, initially at a decreasing rate followed by an increasing rate. The increasing rate of torsional rigidity could be explained by stiffening of the overall structure due to stiffening of the braid. It is possible that the stiffening effect was delayed for the hybrid wire with 55° braid with diamond braid and may come into force at a higher twist angle as the stiffening effect starts first with the 45° braid, followed by the 30° braid then the 55° braid for hybrid wires with regular braid topology. The inelastic behaviour of all configurations of hybrid wires tested under torsion, could also arise due to the inter rod interaction (wrapping around the central rod), giving rise to geometric non linearity. The behaviour of single rods can also be observed in Fig. 11, where the composite rods depicted linear behaviour till the maximum tested limit (400 °/m), however the rods are expected to depict non-linear before failure, as unidirectional fibres in composite rods depict inelastic behaviour in a shear mode of deformation at very high strains.

## 5. Discussion

If the flexural and torsional rigidities of hybrid wires with  $\Phi$  2 mm and 4 mm rods are compared with metallic wires, the advantages of hybrid wires can be observed to be highly significant. The flexural and torsional rigidities of metallic armour wires have been calculated using Eqs. 2 & 5, using the dimensions (30 mm X 1.5 mm)

provided in [33]. The tensile modulus used for carbon steel was 210 GPa obtained from [34], and its shear modulus value of 79 GPa was obtained from [35]. For ease of comparison, mean value of flexural and torsional rigidity have been used for each hybrid wire with  $\Phi$  2 mm and  $\Phi$  4 mm rods.

On comparing the flexural rigidity between the hybrid wires with  $\Phi$  4 mm rods and the traditional (rectangular cross-section) armour wire, an approximate increase of 390% was observed. However, on comparing the flexural rigidity of hybrid wires with  $\Phi$  2 mm rods with the traditional armour wire, an approximate decrease of 69% was observed. If the two types of hybrid wires with different individual rod diameters are compared, an approximate decrease of 94% was observed when  $\Phi$  2 mm rods are incorporated instead of  $\Phi$  4 mm rods in the hybrid wire. This decrease in flexural rigidity highlights one of the advantages of using hybrid wires which is, their flexural rigidity can be tailored by changing their structural parameters.

On comparing the torsional rigidities between two types of hybrid wires ( $\Phi$  2 mm and  $\Phi$  4 mm rods), an approximate decrease of 95% was observed if hybrid wires with  $\Phi$  2 mm rods were employed instead of  $\Phi$  4 mm rods, which again provide tailorability advantage to the hybrid wires. If torsional rigidities of hybrid wire and metallic wires are compared, an approximate decrease of 99.9% was observed if any of the hybrid wires with  $\Phi$  2 mm or  $\Phi$  4 mm rods were used, in place of metallic wires. This is due to the high polar moment of inertia and high shear modulus, of rectangular cross-sectional metallic wires. Very low torsional rigidities of hybrid wires, further add to the advantages of them being better alternative to metallic wires.

## 6. Conclusions

The novel hybrid composite wire design presented in this paper offers many advantages over traditional metallic armour wires:

- The flexural and torsional rigidities of hybrid composite wires can be varied depending upon the curvature of the flexible riser by varying the structural parameters (braid angle, braid topology, or individual rod diameter) during the manufacturing process.
- Bending strains are minimised for the composite components.
- The hybrid wire shows inelastic behaviour under both flexural and torsional deformations with the help of inter-rod interactions, helping to prevent brittle fracture.

Reflecting upon the experimental work carried out in this paper, the effect of individual rod diameters (2 mm and 4 mm) in the hexagonal pack was found to be highly significant on both the flexural and torsional rigidities. The effect of braid angle (30°, 45° and 55°) and braid topology (diamond and regular) upon the flexural rigidity

of the hybrid wire was not significant. However, they did have a significant effect upon the torsional rigidity. The highest torsional rigidity was observed for 45° braid, and regular braid topology. The effect of both braid angle and braid topology was more pronounced in the inelastic region during high deformation loads (torsion and flexural). The hybrid wires with bonded edges showed almost twice the flexural rigidity compared to those with no bonded edges. Due to the ability to tailor hybrid composite wires, they can potentially be a significant alternative to metallic tensile armour wires, though further work, with the help of experimental and computational methods, needs to be carried out to explore the properties of these wires.

### **Acknowledgement**

The authors would like to thank the staff members of University of Manchester (United Kingdom) and GE Oil & Gas (United Kingdom) for all their help and support.

### **References**

1. Fergestad D, Løvteit SA. Handbook on Design and Operation of Flexible Pipes: MARINTEK / NTNU / 4Subsea, 2014.
2. Salama MM. Advance Composites For The Offshore Industry: Applications and Challenges. Composite Material for Offshore Operations: Proceedings of the First International Workshop. Houston, Texas, 1993.
3. Mekha BB. New Frontiers in the Design of Steel Catenary Risers for Floating Production Systems. Journal of Offshore Mechanics and Arctic Engineering. 2001; 123: 153-8.
4. Sævik S. Theoretical and experimental studies of stresses in flexible pipes. Computers & Structures. 2011; 89: 2273-91.
5. de Sousa JRM, Campello GC, Kwietniewski CEF, Ellwanger GB, Strohaecker TR. Structural response of a flexible pipe with damaged tensile armor wires under pure tension. Marine Structures. 2014; 39: 1-38.
6. Institute AP. Practice For Flexible Pipe. AN-SI/API Recommended Practice 17B. 4th ed; 2007.
7. Executive H&S. Guidelines for integrity monitoring of Unbonded flexible pipe - OTO 98108. Health and Safety Executive; 1998.
8. Clarke T, Jacques R, Bisognin A, Camerini C, Damasceno S, Strohaecker T. Monitoring the structural integrity of a flexible riser during a full-scale fatigue test. Engineering Structures. 2011; 33: 1181-6.
9. Désamais N, Félix-Henry A, Taravel-Condat C, Drouës A. Use of High Strength Steel Wires For Flexible Pipe In Low Sour Service Conditions: Impact On Deep Water Applications. The Seventeenth International



- Offshore and Polar Engineering Conference. Lisbon, Portugal: International Society of Offshore and Polar Engineers; 2007. p. 1033-8.
10. Kalman M, Belcher J. Flexible Risers with Composite Armor for Deep Water Oil and Gas Production. Composite Materials for Offshore Operations. S. S. Wang, J. G. Williams, and K. H. Lo, Eds., American Bureau of Shipping; 1999. p. 165-179.
  11. Do AT, Lambert A. Qualification of Unbonded Dynamic Flexible Riser With Carbon Fibre Composite Armors. Offshore Technology Conference; 2012.
  12. Do AT, Bernard G, Hanonge D. Carbon Fiber Armors Applied to Presalt Flexible Pipe Developments. Offshore Technology Conference. Houston, Texas, USA; 2013.
  13. Jha V, Finch D, Dodds N, Latta J. Optimized Hybrid Composite Flexible Pipe for Ultra-Deepwater Application. 34th International Conference on Ocean, Offshore and Arctic Engineering. St. John's, Newfoundland, Canada: ASME; 2015.
  14. N. Ismail RN, and M. Kanarellis. Design consideration for selection of flexible riser configuration. Offshore and Arctic Operations. 1992;42.
  15. Qiang B, Yong B. Subsea Pipelines and Risers. London: Elsevier, 2005.
  16. Zureick A, Scott D. Short-Term Behavior and Design of Fiber-Reinforced Polymeric Slender Members under Axial Compression. Journal of Composites for Construction. 1997;1:140-9.
  17. Potluri P, Rawal A, Rivaldi M, Porat I. Geometrical modelling and control of a triaxial braiding machine for producing 3D preforms. Composites Part A: Applied Science and Manufacturing. 2003; 34: 481-92.
  18. Branscomb D, Beale D, Broughton R. New Directions in Braiding. Journal of Engineered Fibres and Fabrics. 2013; 8:11-24.
  19. ASTM, Standard Test Method for Tensile Properties of Pultruded Glass-Fiber-Reinforced Plastic Rod - D3916, Annual Book of ASTM Standards; 2002.
  20. Bezdek A, Kuperberg W. Maximum density Space Packing with Congruent Circular Cylinders of Infinite Length, *Mathematika*. 1990; 37: 74-80.
  21. Starostin EL. On the perfect hexagonal packing of rods. *Journal of Physics: Condensed Matter*. 2006; 18: 187-204.
  22. Zhang Q, Beale D, Adanur S, Broughton RM, Walker RP. Structural Analysis of a Two- dimensional Braided Fabric *Journal of Textile Institute*. 1997; 88: 41-52.

23. ASTM. Standard Test Methods for Flexural Properties of Unreinforced and Reinforced Plastics and Electrical Insulating Materials - D790; Annual Book of ASTM Standards; 2003.
24. ASTM. Standard Test Method for Flexural Properties of Unreinforced and Reinforced Plastics and Electrical Insulating Materials by Four-Point Bending - D6272; Annual Book of ASTM Standards; 2003.
25. ASTM. Flexural Properties of Polymer Matrix Composite Materials - D7264/D7264M. Annual Book of ASTM Standards; 2007.
26. ASTM. Standard Test Method for Flexural Properties of Fiber Reinforced Pultruded Plastic Rods - D4476. Annual Book of ASTM Standards; 2006.
27. Rivin E. Stiffness and Damping in Mechanical Design: CRC Press, 1999.
28. ASTM. Standard Test Method for In-Plane Shear Response of Polymer Matrix Composite Materials by Tensile Test of a  $\pm 45^\circ$  Laminate - D 3518/D 3518M Annual Book of ASTM Standards; 2001.
29. ASTM. Standard Test Method for Inplane Shear Properties of Hoop Wound Polymer Matrix Composite Cylinders - D5448/D5448. Annual Book of ASTM Standards; 2000.
30. Ahmadi MS, Johari MS, Sadighi M, Esfandeh M. An experimental study on mechanical properties of GFRP braid-pultruded composite rods. *eXPRESS Polymer Letters*. 2009; 3: 560-8.
31. Pipes RB, Pagano NJ. Interlaminar Stresses in Composite Laminates Under Uniform Axial Extension. *Journal of Composite Materials*. 1970; 4: 538-48.
32. Potluri P, Manan A, Francke M, Day RJ. Flexural and torsional behaviour of biaxial and triaxial braided composite structures. *Composite Structures*. 2006; 75: 377-86.
33. Witz JA. A Case Study in the Cross-section Analysis of Flexible Risers. *Marine Structures*. 1996;9:885-904.
34. Franssen J-M, Real PV. Annex C: Mechanical Properties of Carbon Steel and Stainless Steel. *Fire Design of Steel Structures: Wiley-VCH Verlag GmbH & Co. KGaA*; 2010. p. 359-81.
35. Collins JA, Busby H, Staab G. Chapter 3 - Materials Selection. *Mechanical Design of Machine Elements and Machines*. 2nd ed; 2010.

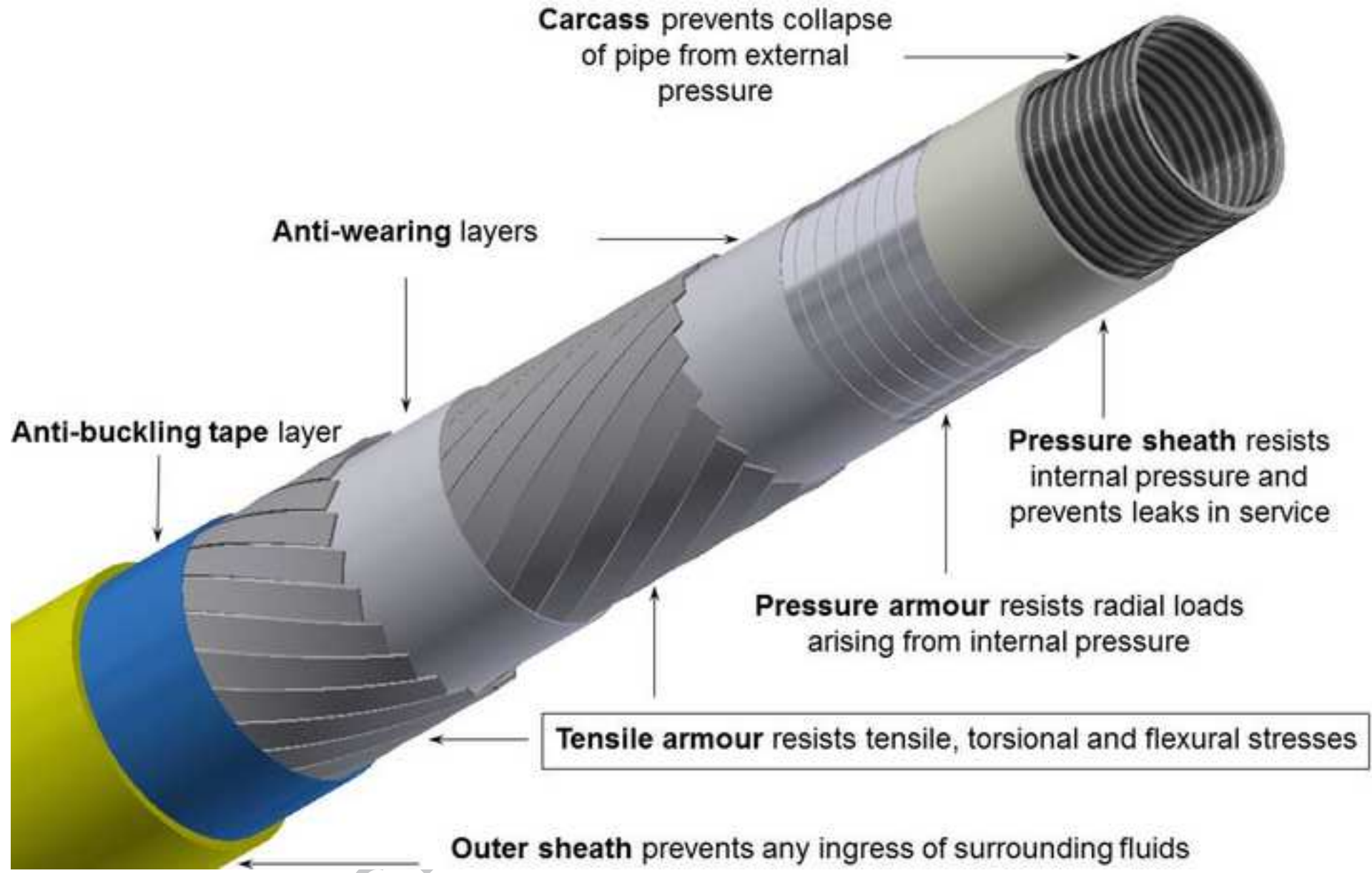
### Image Captions

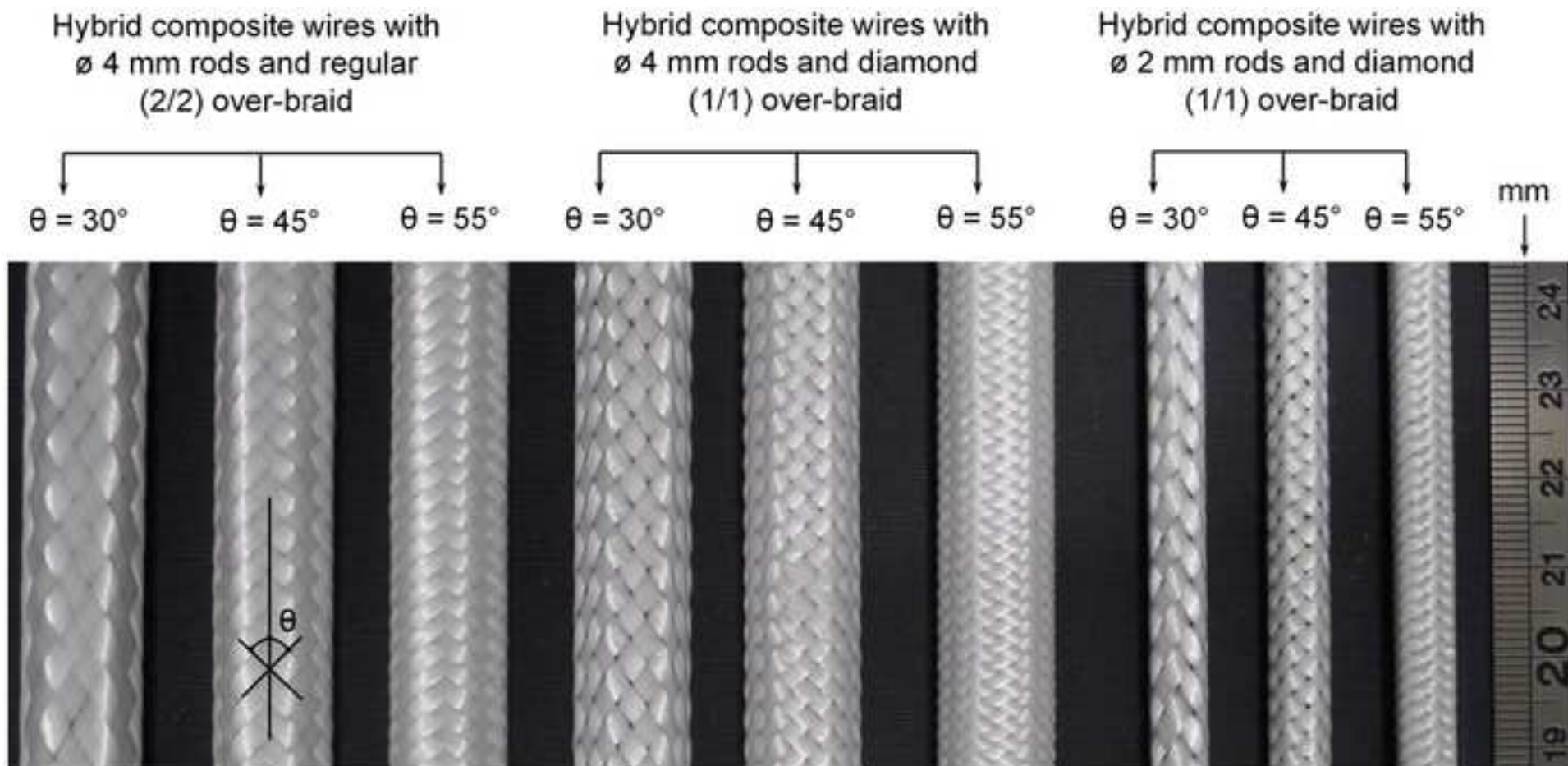
1. Fig. 1: Function of different layers in a flexible riser
2. Fig. 2: Different configuration examples of hybrid composite wires

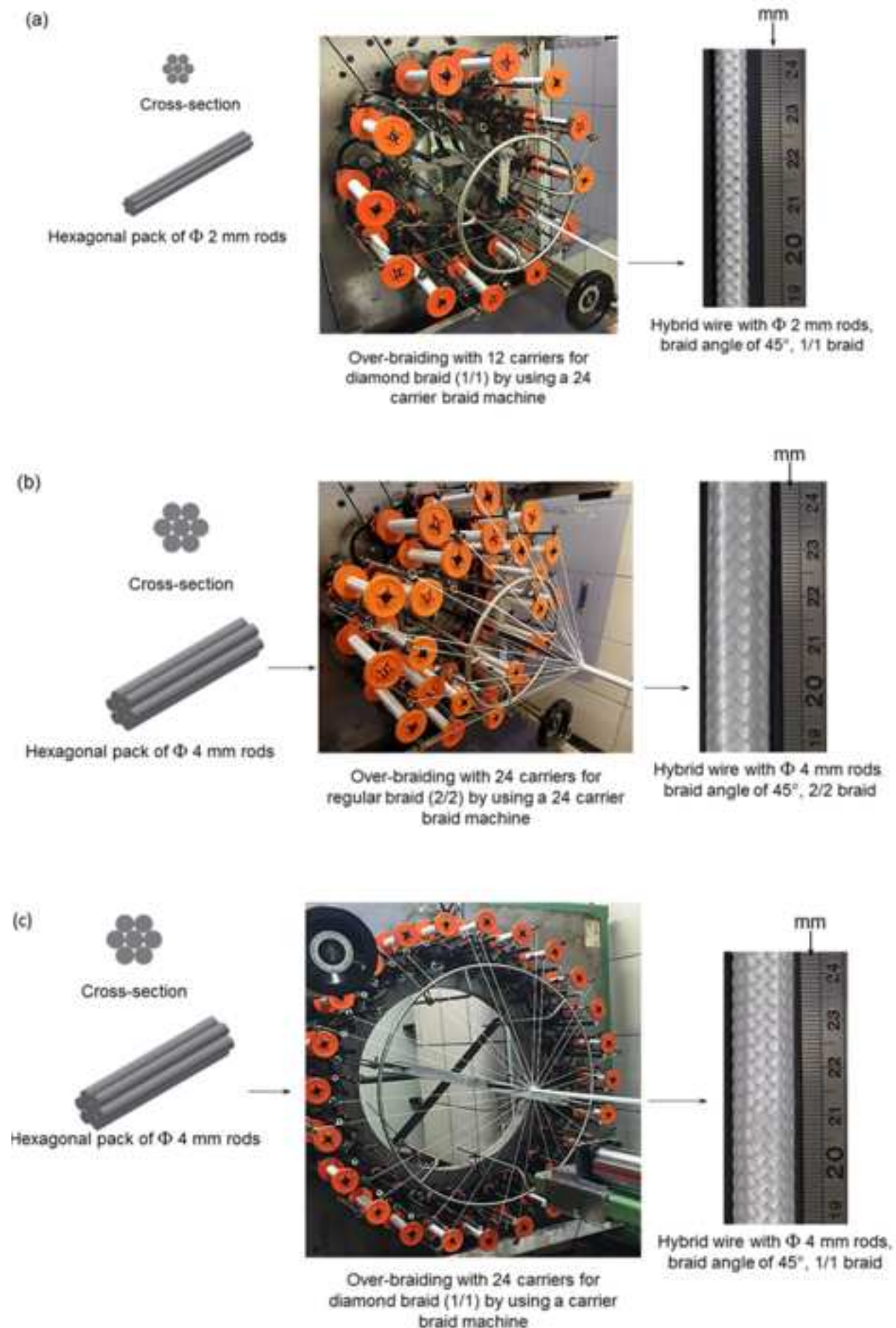
3. Fig. 3: Over-braiding process
4. Fig. 4: Hybrid composite wire (with  $\Phi$  2 mm rods, braid angle of  $30^\circ$ , and diamond braid topology) in a four-point flexural test setup
5. Fig. 5: Torsion test to maximum limit of  $40^\circ$  twist angle for: (a) hybrid wire ( $45^\circ$  braid angle, 1/1 braid topology) with  $\Phi$  2 mm rods and (b) hybrid wire ( $45^\circ$  braid angle, 2/2 braid topology) with  $\Phi$  4 mm rods
6. Fig. 6: Normalised flexural rigidity of hybrid wires with respect to individual rod used in the packing
7. Fig. 7: Normalised (values of y axis divided by actual peak bending moment) flexural behaviour of hybrid wires and individual rods for: (a)  $\Phi$  2 mm rods and (b)  $\Phi$  4 mm rods
8. Fig. 8: Four point flexural test on hybrid composite wires (with  $\Phi$  4 mm rods and regular braid topology) for: (a)  $30^\circ$  and (b)  $45^\circ$  braid angles.
9. Fig. 9: Effect of boundary condition for: (a) hybrid wire without braid (taped edges), (b) hybrid wire without braid (bonded edges), (c) hybrid wire ( $45^\circ$ , 2/2, taped edges), and (d) hybrid wire ( $45^\circ$ , 2/2, unbonded edges)
10. Fig.10: Effect of point loads using normalised flexural rigidities of hybrid wire (1/1,  $\Phi$  4 mm) with respect to 4 point flexural tests.
11. Fig. 11: Normalised (values of y axis divided by maximum actual torque value) torsional behaviour of hybrid wires and individual rods for: (a)  $\Phi$  2 mm rods and (b)  $\Phi$  4 mm rods

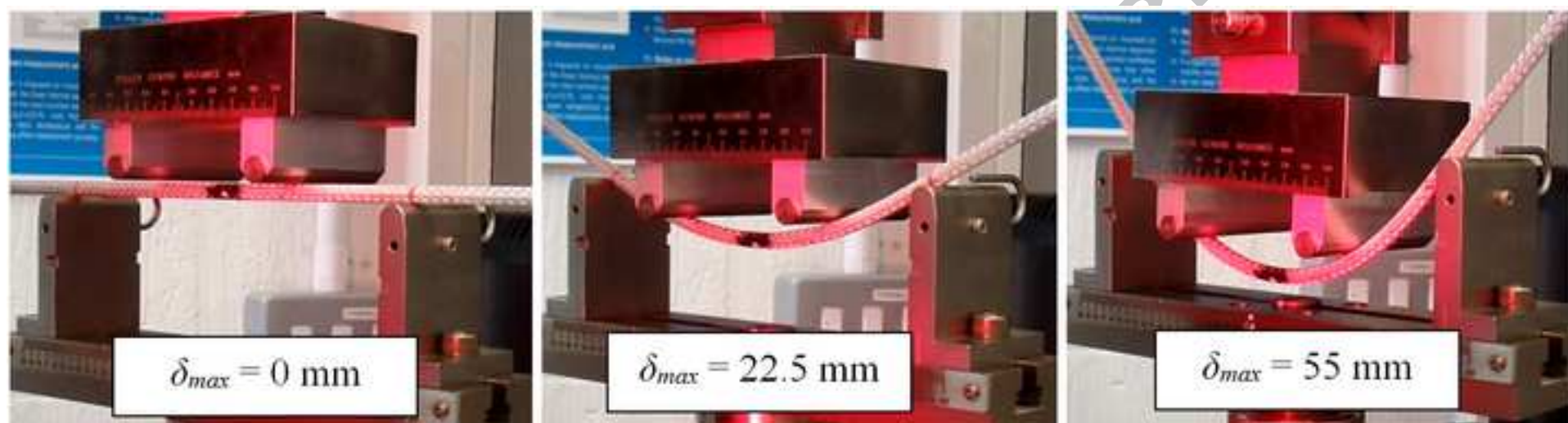
#### Table Captions

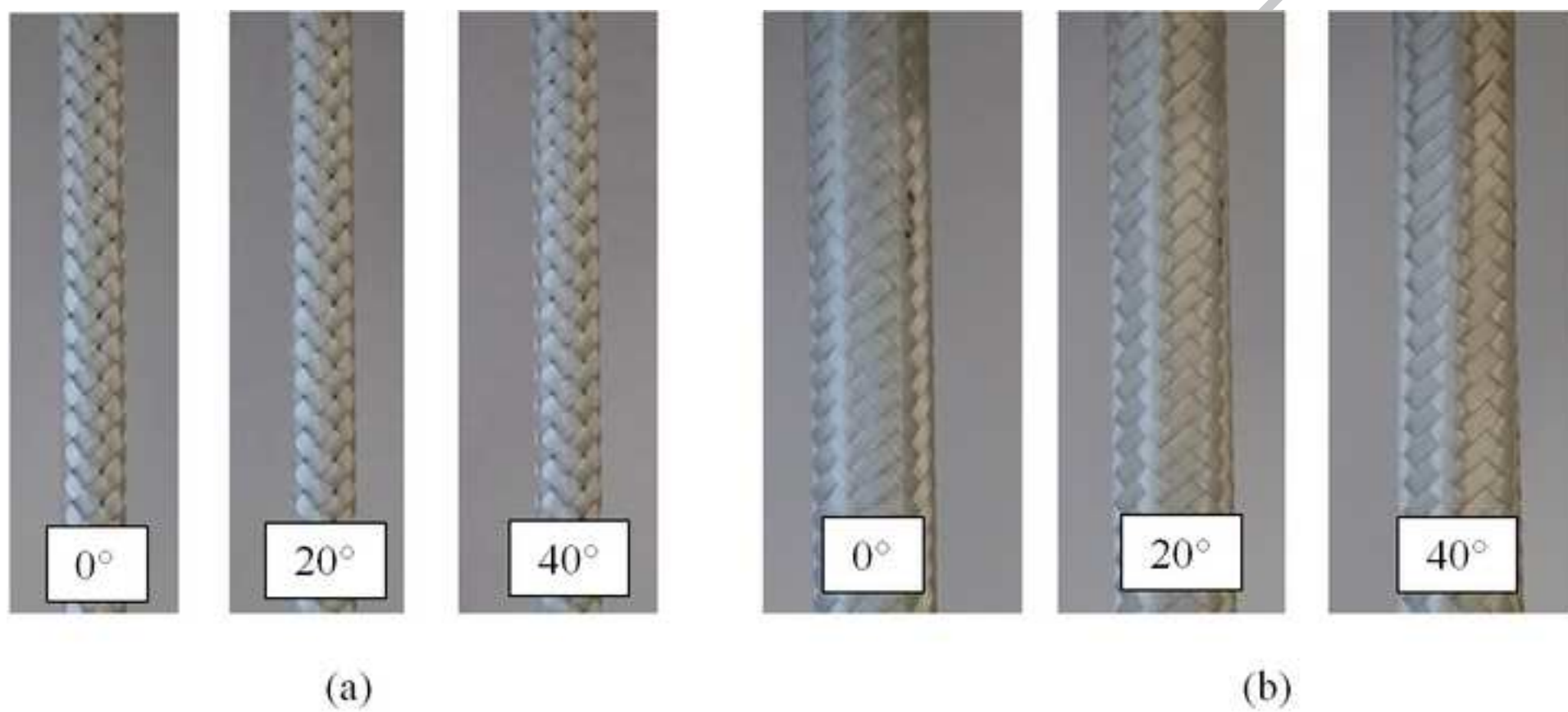
1. Table 1: Material properties
2. Table 2: Structural properties of braid



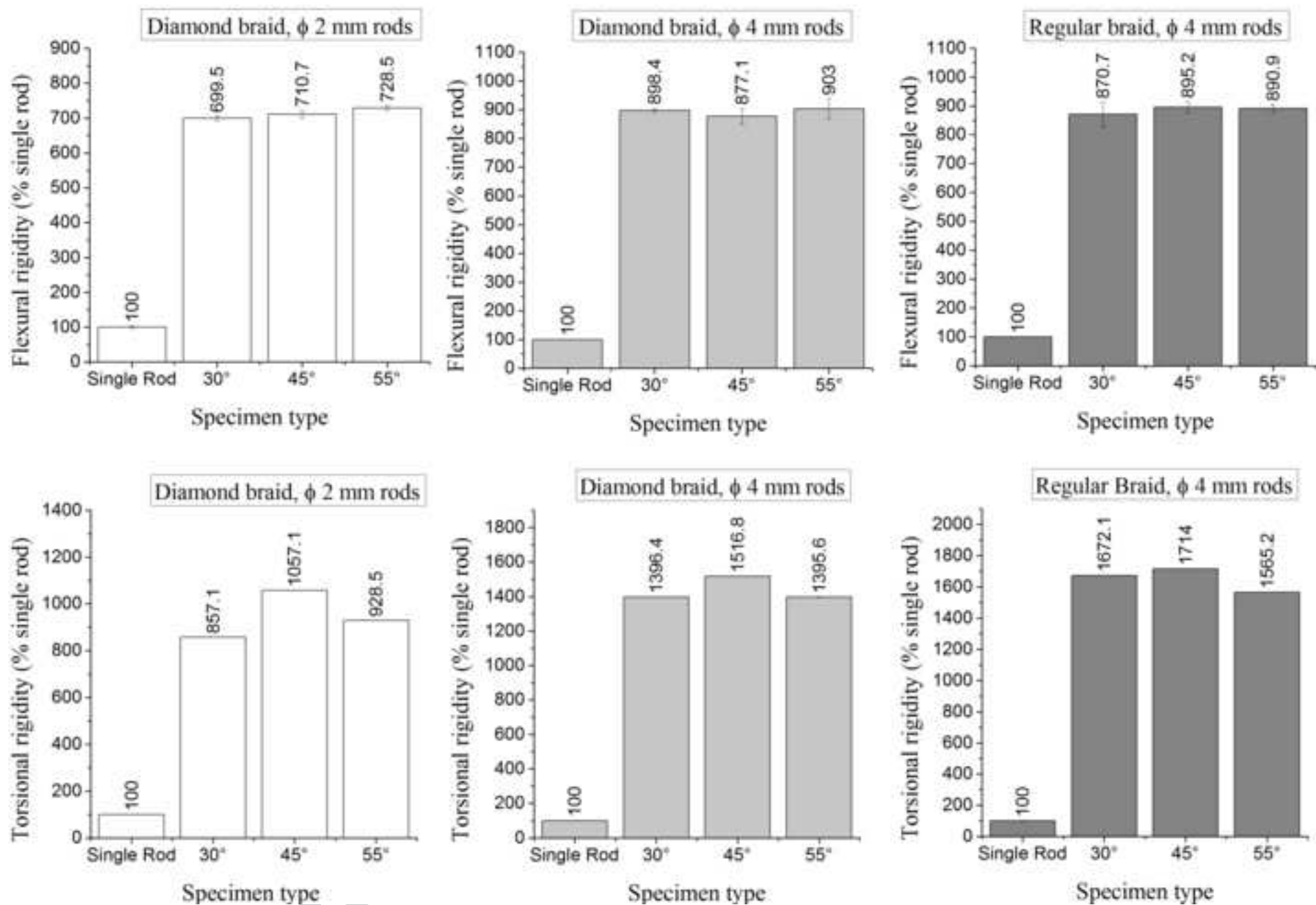


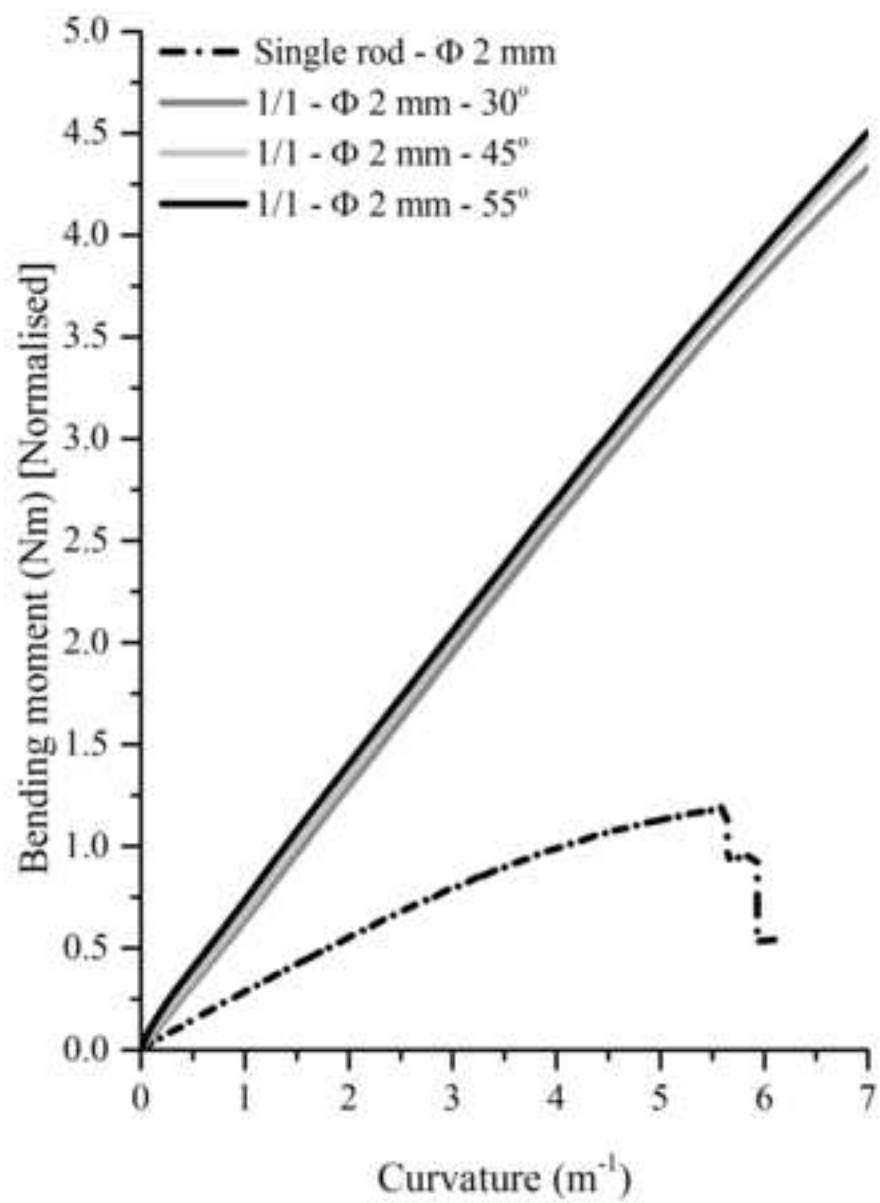




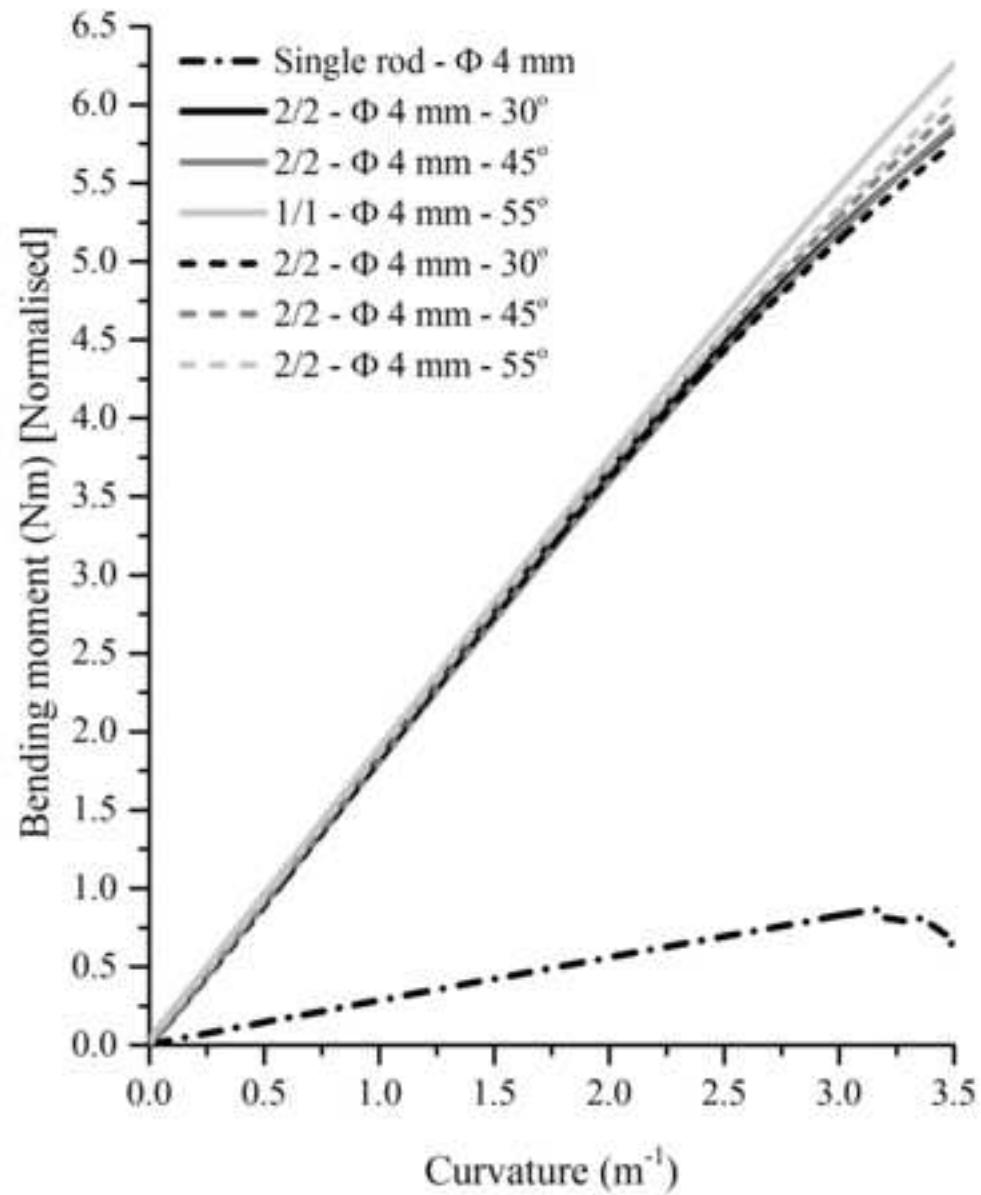




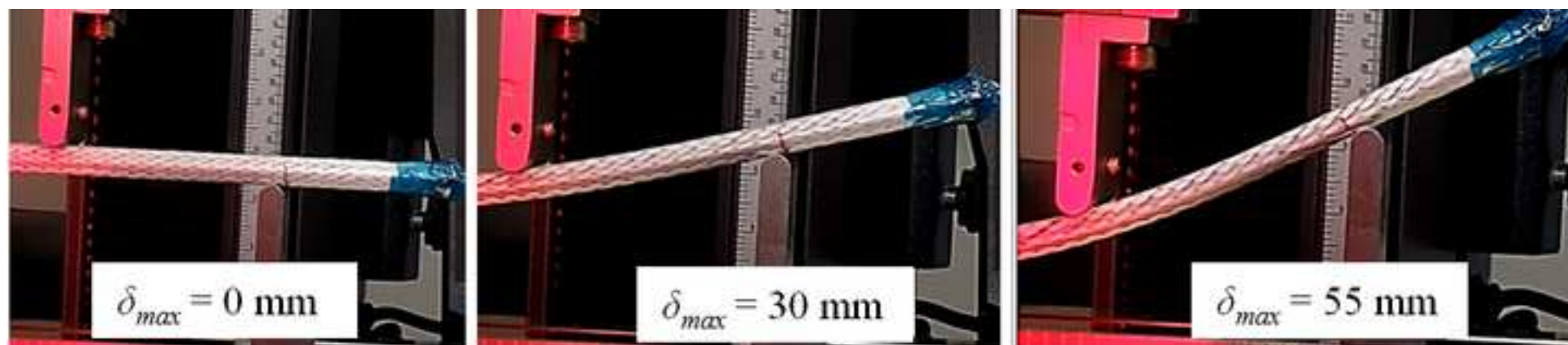




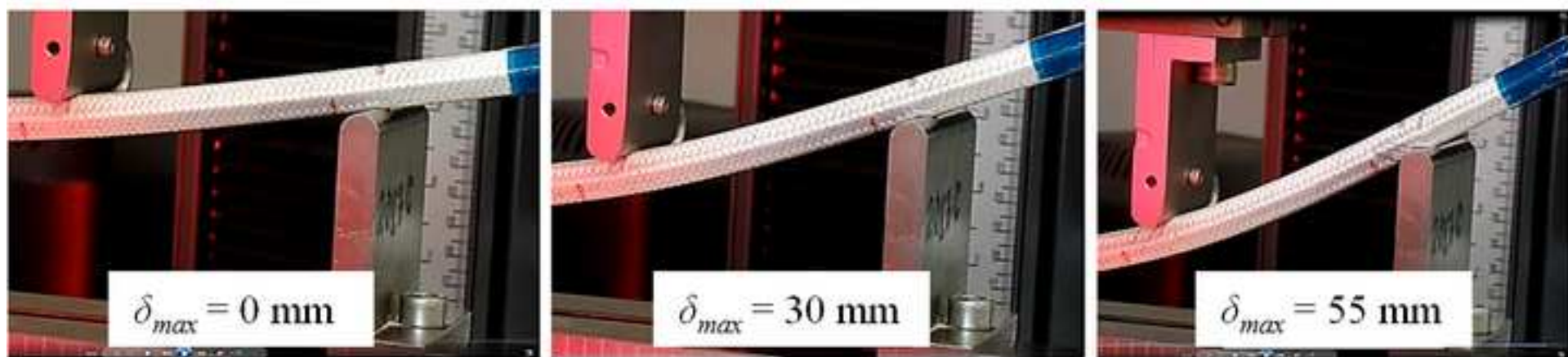
(a)



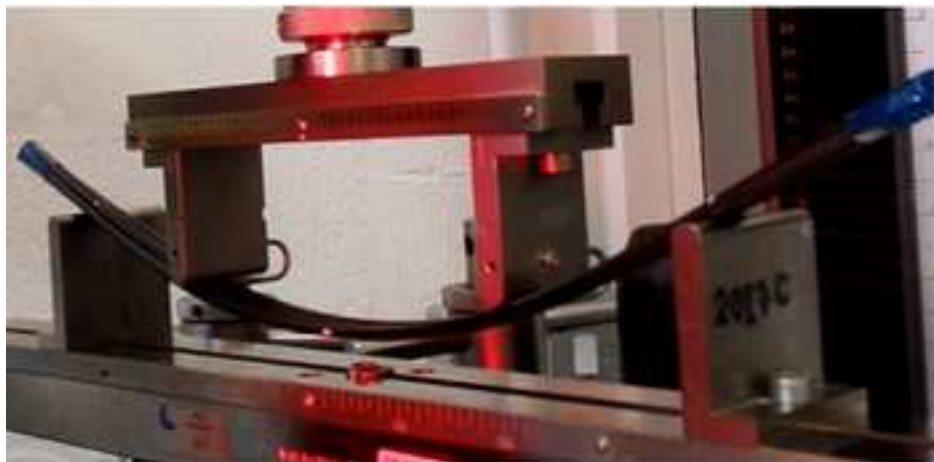
(b)



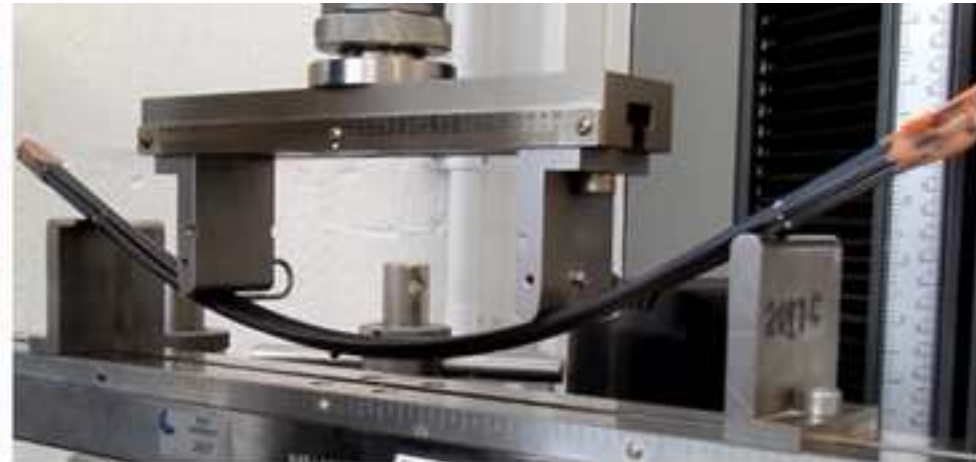
(a)



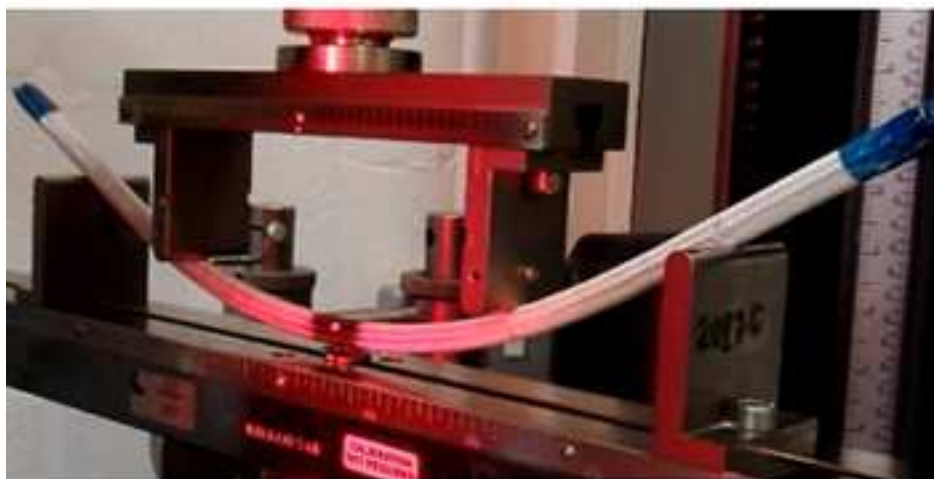
(b)



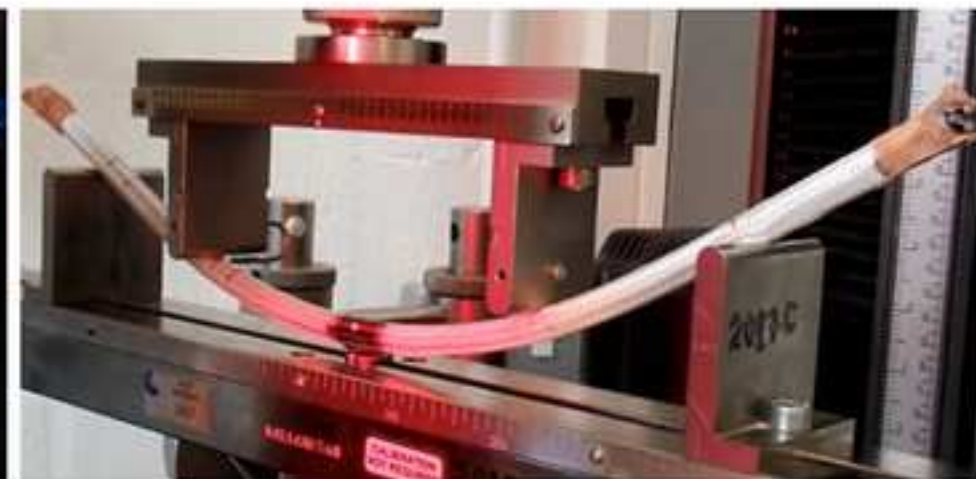
(a)



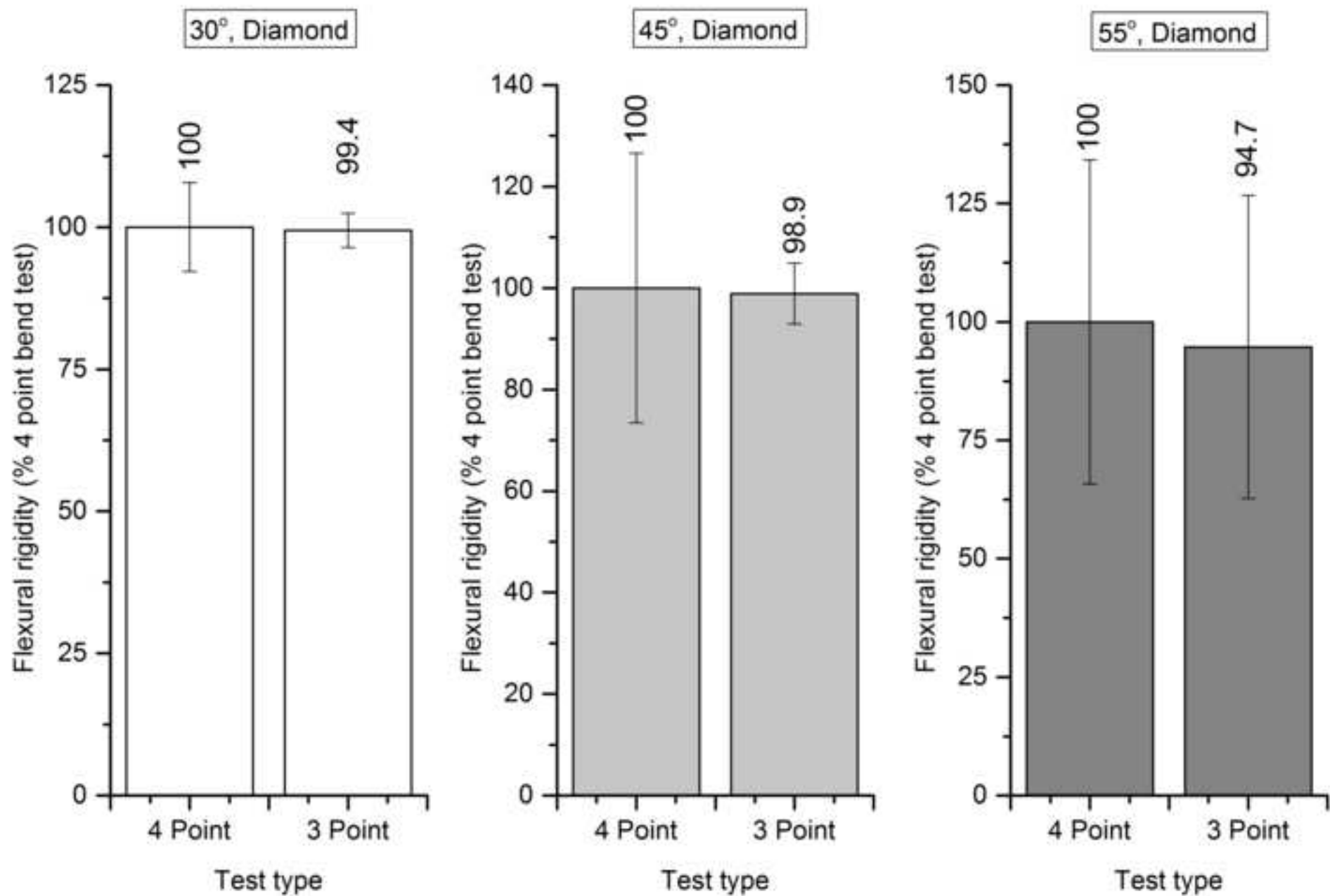
(b)

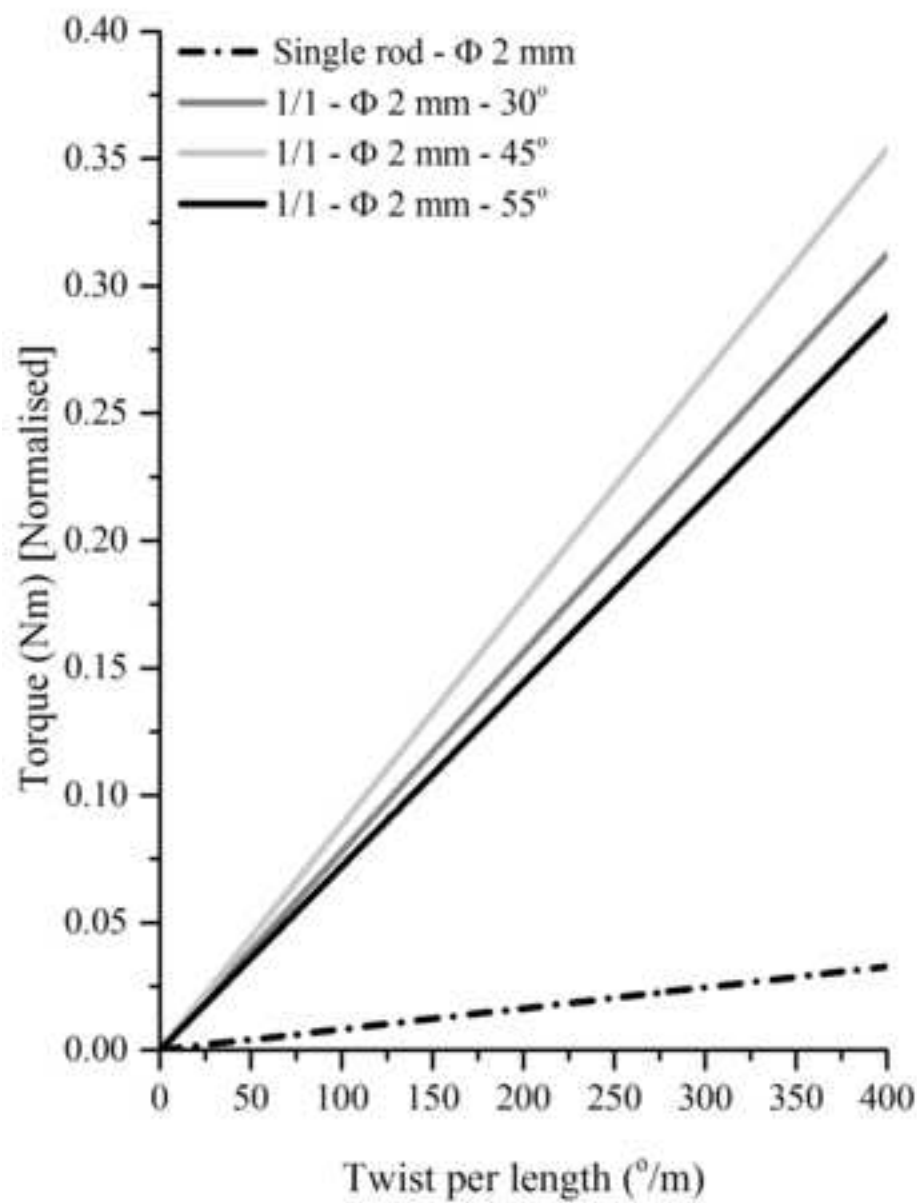


(c)

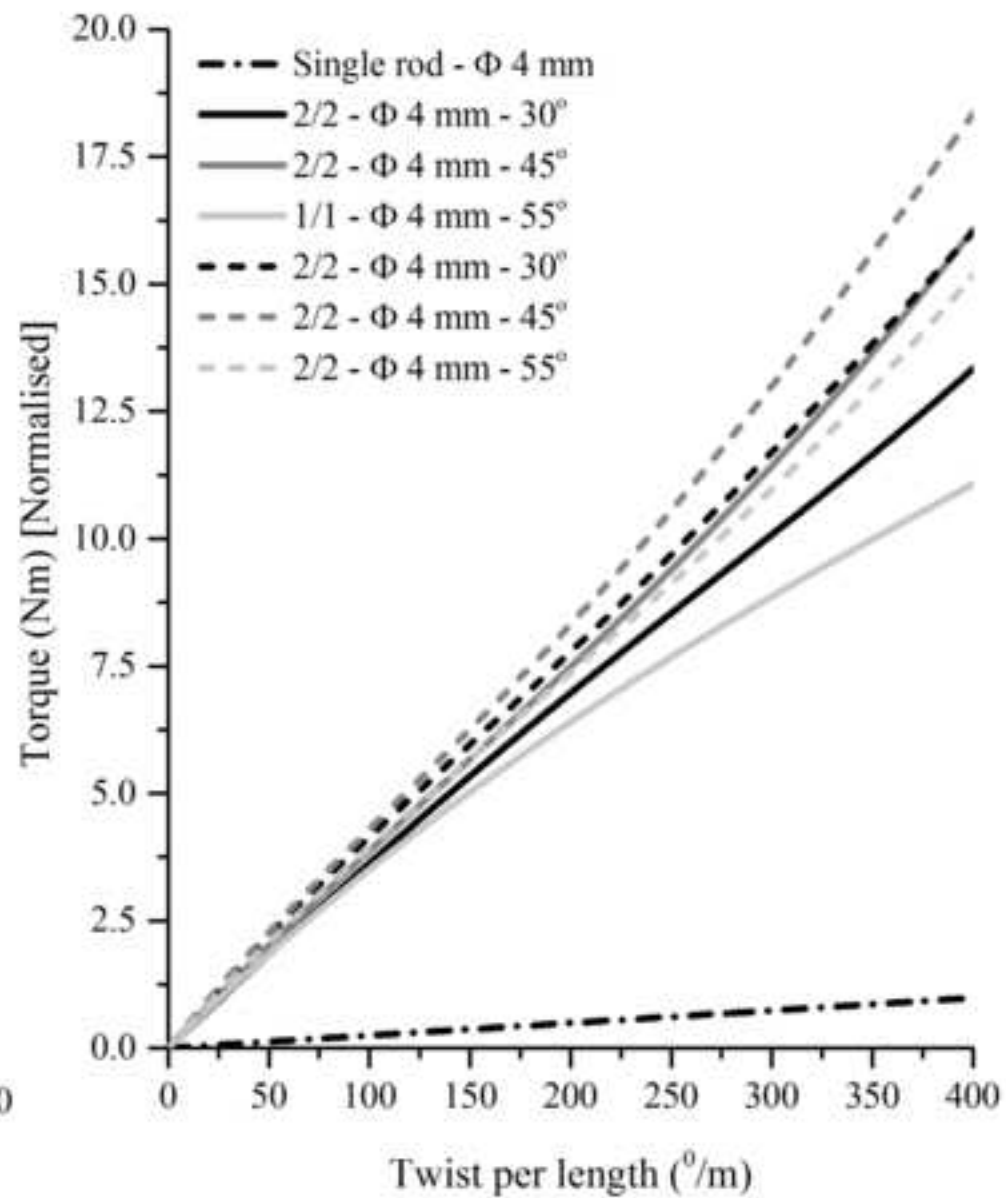


(d)





(a)



(b)

| <i>Material</i>               | <i>Density (g/cm<sup>3</sup>)</i> | <i>Tensile modulus (GPa)</i> |
|-------------------------------|-----------------------------------|------------------------------|
| <i>Circular pultruded rod</i> | <i>1.03 ± 0.45</i>                | <i>110 ± 12</i>              |
| <i>Braid tow</i>              | <i>0.97</i>                       | <i>210</i>                   |

*± Standard deviation*

ACCEPTED MANUSCRIPT

| $\Phi$<br>(mm) | Braid<br>topology | Braid angle<br>( $\theta^\circ$ ) | Braid crimp<br>(%) | Braid thickness<br>(mm) | Tow width<br>(mm) |
|----------------|-------------------|-----------------------------------|--------------------|-------------------------|-------------------|
| 2              | 1/1               | 30                                | $2.16 \pm 0.41$    | $0.32 \pm 0.02$         | $2.53 \pm 0.05$   |
| 2              | 1/1               | 45                                | $3.38 \pm 0.45$    | $0.41 \pm 0.07$         | $1.99 \pm 0.03$   |
| 2              | 1/1               | 55                                | $4.56 \pm 0.56$    | $0.49 \pm 0.09$         | $1.46 \pm 0.01$   |
| 4              | 1/1               | 30                                | $3.23 \pm 0.34$    | $0.31 \pm 0.01$         | $2.61 \pm 0.06$   |
| 4              | 1/1               | 45                                | $3.62 \pm 0.28$    | $0.40 \pm 0.08$         | $1.98 \pm 0.08$   |
| 4              | 1/1               | 55                                | $6.48 \pm 0.79$    | $0.48 \pm 0.07$         | $1.55 \pm 0.04$   |
| 4              | 2/2               | 30                                | $2.64 \pm 0.39$    | $0.32 \pm 0.05$         | $3.47 \pm 0.06$   |
| 4              | 2/2               | 45                                | $3.61 \pm 0.45$    | $0.38 \pm 0.04$         | $2.45 \pm 0.01$   |
| 4              | 2/2               | 55                                | $5.55 \pm 0.46$    | $0.46 \pm 0.06$         | $1.95 \pm 0.04$   |